

Coherent Structures in Weakly-birefringent Nonlinear Optical Fibers

Jianke Yang
Department of Mathematics and Statistics
The University of Vermont
Burlington, VT 05401

This paper studies two coupled nonlinear Schrödinger equations which govern the pulse propagation in weakly-birefringent nonlinear optical fibers. The coherent structures for these equations, such as vector solitons and localized oscillating solutions, are studied analytically and numerically. Three types of localized oscillating structures are identified and their functional forms determined by perturbation methods. In some of these structures, infinite oscillating tails are present. The implications of these tails are also discussed.

1 Introduction

In recent years, the propagation of pulses in a nonlinear optical fiber has received extensive study. In a single-mode optical fiber, when third-order nonlinear effects are included, pulse propagation is described approximately by the nonlinear Schrödinger equation. This equation is completely integrable [1] and solitons exist in certain cases. Since solitons can propagate without dispersion, it has been proposed that they be used as information bits in long-distance optical communication systems. But, a single-mode optical fiber is not really “single-mode”. It is actually bi-modal due to the presence of birefringence. Birefringence tends to split a pulse into two pulses in the two polarization directions, but nonlinear effects can trap them together against splitting. Menyuk [2] showed that the two polarization components in a birefringent optical fiber are governed by two coupled nonlinear Schrödinger-type equations. In the case of high birefringence, the difference in the two phase velocities has no overall effect on the average. The equations can be readily converted into two coupled nonlinear Schrödinger equations which have been extensively studied ([3], [4], [5], [6]). It was found that for the Kerr nonlinearity, vector solitons of arbitrary polarizations exist that can propagate without distortion. These vector solitons can undergo internal oscillations if they are disturbed. In the low birefringence case, the difference in the group velocities can be ignored, but the difference in the phase velocities should still be taken into account. It was found that only very special vector solitons can be stable ([7], [8]). In general, energy injected into one polarization component can switch to the other, and non-dispersive, energy-sharing pulses are formed ([7],

[9]). These pulses can also travel over long distances, but their shapes keep changing periodically. Currently, for these energy-sharing pulses, some numerical results are available, but little analytical investigation has been made.

In this paper, the pulse propagation in weakly-birefringent nonlinear optical fibers is studied mainly by analytical methods. The relevant equations are ([2], [9])

$$iA_t + A_{xx} + \kappa B + (AA^* + \beta BB^*)A = 0, \quad (1.1a)$$

$$iB_t + B_{xx} + \kappa A + (BB^* + \beta AA^*)B = 0, \quad (1.1b)$$

where A and B are linearly related to the slowly varying wave envelopes of the two polarization components, and the roles of x and t have been switched for convenience. κ and β are real-valued coefficients. For Kerr nonlinearity, $\beta = 2$. But β can take other values depending on the nature of the anisotropy. When $\kappa = 0$, (1.1) becomes the coupled nonlinear Schrödinger equations which have been studied before. In this paper, κ and β are arbitrary parameters, but it is assumed that $\kappa \neq 0$. The system (1.1) in general is not completely integrable, so we focus on its coherent structures such as vector solitons and, in particular, localized oscillating structures. Vector solitons will be determined numerically for the most part, while localized oscillating structures will be determined analytically by perturbation methods. The knowledge of these coherent structures hopefully will shed light on the pulse propagation and the design of such communication systems.

It should be noted that equations (1.1) arise in other situations as well. For instance, the coupling between two waveguide modes in a directional coupler is governed by (1.1) with $\beta = 0$. In this case, soliton switching and propagation has been studied by Chu et al. [10] using the variational principle. They assumed that the solutions take a particular ansatz. Inserting it into the Lagrangian density, they obtained the ordinary differential equations for the evolution of the parameters in the assumed ansatz. They found good agreement between their analytical results and numerical ones. But their assumption of the solution profile is a little artificial and could not be justified in general. In the present paper, the full solution dynamics for soliton switching is determined by perturbation methods. These results provide much insight into the dynamics of the solution structures. They may also be used to rationalize the solution profiles assumed by Chu et al. in their variational principle approach. The trade-off is that these perturbation solutions are valid only when β and κ are near some special values. Nonetheless, they are very helpful in the understanding of the pulse propagation in the weakly-birefringent nonlinear optical fibers.

2 Vector Solitons (Permanent Waves)

It is well known that vector solitons of the form

$$A = e^{i\frac{U}{2}x + i(\omega - \frac{U^2}{4})t} r_1(\xi), \quad (2.1a)$$

$$B = e^{i\frac{U}{2}x + i(\omega - \frac{U^2}{4})t} r_2(\xi) \quad (2.1b)$$

exist in equations (1.1), where $\xi = x - Ut$ and $r_1(\xi), r_2(\xi)$ are real-valued functions. After a scaling of variables

$$\bar{\xi} = \sqrt{\omega} \xi, \quad \bar{\kappa} = \frac{\kappa}{\omega}, \quad \bar{r}_1 = \frac{r_1}{\sqrt{\omega}}, \quad \bar{r}_2 = \frac{r_2}{\sqrt{\omega}} \quad (2.2)$$

and the bars dropped, r_1 and r_2 are found to satisfy the following equations

$$r_{1\xi\xi} - r_1 + \kappa r_2 + (r_1^2 + \beta r_2^2)r_1 = 0, \quad (2.3a)$$

$$r_{2\xi\xi} - r_2 + \kappa r_1 + (r_2^2 + \beta r_1^2)r_2 = 0. \quad (2.3b)$$

In order for r_1 and r_2 to exponentially decay as $|\xi| \rightarrow \infty$, it is necessary that $-1 < \kappa < 1$. Some special solutions can be readily obtained. For instance,

$$r_1 = r_2 = \sqrt{\frac{2(1-\kappa)}{1+\beta}} \operatorname{sech} \sqrt{1-\kappa} \xi \quad (2.4)$$

and

$$r_1 = -r_2 = \sqrt{\frac{2(1+\kappa)}{1+\beta}} \operatorname{sech} \sqrt{1+\kappa} \xi \quad (2.5)$$

are solutions of (2.3). When κ is small, assume that $r_1 = O(1)$ and $r_2 = O(\kappa)$, then

$$r_{1\xi\xi} - r_1 + r_1^3 \approx 0. \quad (2.6)$$

If we take

$$r_1 \approx \sqrt{2} \operatorname{sech} \xi, \quad (2.7)$$

then r_2 is determined approximately by the equation

$$r_{2\xi\xi} + (2\beta \operatorname{sech}^2 \xi - 1)r_2 \approx -\sqrt{2} \kappa \operatorname{sech} \xi. \quad (2.8)$$

A unique localized r_2 solution always exists if $\beta \neq 1$. For instance, when $\beta = 0$,

$$r_2 \approx \frac{\sqrt{2}}{2} \kappa \int_0^\infty \{\operatorname{sech}(u + \xi) + \operatorname{sech}(u - \xi)\} e^{-u} du. \quad (2.9)$$

When $\beta = 1.5$, the solution of the equation (2.8) is numerically determined and plotted in Figure 4. The general solutions of (2.3) can be effectively determined numerically. Notice that a variable transform

$$f_1 = \frac{1}{2}(r_1 + r_2), \quad f_2 = \frac{1}{2}(r_1 - r_2) \quad (2.10)$$

reduces equations (2.3) to the form

$$f_{1\xi\xi} - (1 - \kappa)f_1 + (\beta + 1)(f_1^2 + \frac{3 - \beta}{1 + \beta} f_2^2)f_1 = 0, \quad (2.11a)$$

$$f_{2\xi\xi} - (1 + \kappa)f_2 + (\beta + 1)(f_2^2 + \frac{3 - \beta}{1 + \beta} f_1^2)f_2 = 0. \quad (2.11b)$$

Numerical solutions of (2.11) can be found in Yang and Benney [3], Yang [6] and Akhmediev et al. [8]. In general, the number of solutions is infinite for any fixed values of κ and β .

The stability of these vector solitons has been investigated by Wright et al. [7] and Akhmediev et al. [8]. Wright et al. showed that the special solutions (2.4) and (2.5) are stable when κ and β

are in the stability region specified in their paper. Akhmediev et al.'s results suggest that vector solitons other than (2.4) and (2.5) are all unstable. The vector solitons (2.4) and (2.5) require A and B to have the same phase and amplitude and are very special. Thus, for an arbitrary initial condition, the end state of the solution, in general, can rarely be such vector solitons but, rather, some other coherent structures which we will study in the next section.

It should be noted that even though most vector solitons (2.1) are unstable, if their instability growth rates are small, they can still travel for a long time without distortion. For instance, when $\kappa \ll 1$, the special vector soliton (2.7), (2.8) has a very small instability growth rate. So it can sustain for a long time, which is confirmed by Wright et al.'s numerical results.

3 Localized Oscillating Structures

A different kind of coherent structure, namely localized oscillating structure, is more important in the system (1.1). As has been indicated in the last section, only very special vector solitons can be stable. Most vector solitons are unstable. They usually disintegrate and evolve into localized oscillating structures. This has been confirmed by the numerical results in [7], [9] and [10].

Little has been known about these localized oscillating structures except some numerical evidence. When $\beta = 0$, Chu et al. [10] studied such structures using the variational principle. Although their results shed some light on the energy-switching properties of these oscillating solutions, their assumption on the profile of these solutions is artificial and can not be justified. The functional forms and dynamics of evolution of these structures are still not clear.

In this section we are going to identify three such structures and determine their functional forms and evolution by perturbation methods. These results will enable us to penetrate into such structures and enhance our understanding of them.

3.1 Oscillating Structures with One Dominant Frequency

When κ is small and β close to 1, oscillating structures can be constructed perturbatively as follows.

Suppose $\kappa = \epsilon k$ and $\beta = 1 + \epsilon b$ where $\epsilon \ll 1$ and $k, b = O(1)$. Then equations (1.1) can be reorganized as

$$iA_t + A_{xx} + (AA^* + BB^*)A = -\epsilon(kB + bBB^*A), \quad (3.1a)$$

$$iB_t + B_{xx} + (BB^* + AA^*)B = -\epsilon(kA + bAA^*B). \quad (3.1b)$$

When $\epsilon = 0$,

$$A(x, t) = \phi_1 \operatorname{sech} x e^{it}, \quad B(x, t) = \phi_2 \operatorname{sech} x e^{it} \quad (3.2)$$

are vector soliton solutions of (3.1) where ϕ_1 and ϕ_2 are complex constants and $|\phi_1|^2 + |\phi_2|^2 = 2$. When ϵ is non-zero but small, solutions can be expanded as perturbation series

$$A = e^{it} \{ \phi_1(T) \operatorname{sech} x + \epsilon A_1(x, T, \epsilon) + \dots \}, \quad (3.3a)$$

$$B = e^{it} \{ \phi_2(T) \operatorname{sech} x + \epsilon B_1(x, T, \epsilon) + \dots \} \quad (3.3b)$$

where $T = \epsilon t$ is the slow-time scale. Notice that these solutions have one dominant frequency 1.

At order 1, it is found that

$$|\phi_1(T)|^2 + |\phi_2(T)|^2 = 2, \quad (3.4)$$

which is expected. At order ϵ ,

$$A_{1xx} - A_1 + \{ (2|\phi_1|^2 + |\phi_2|^2)A_1 + \phi_1^2 A_1^* + \phi_1 \phi_2^* B_1 + \phi_1 \phi_2 B_1^* \} \operatorname{sech}^2 x = F_1, \quad (3.5a)$$

$$B_{1xx} - B_1 + \{ (2|\phi_2|^2 + |\phi_1|^2)B_1 + \phi_2^2 B_1^* + \phi_2 \phi_1^* A_1 + \phi_1 \phi_2 A_1^* \} \operatorname{sech}^2 x = F_2, \quad (3.5b)$$

where

$$F_1 = -i\phi_{1T} \operatorname{sech} x - k\phi_2 \operatorname{sech} x - b|\phi_2|^2 \phi_1 \operatorname{sech}^3 x, \quad (3.6a)$$

$$F_2 = -i\phi_{2T} \operatorname{sech} x - k\phi_1 \operatorname{sech} x - b|\phi_1|^2 \phi_2 \operatorname{sech}^3 x. \quad (3.6b)$$

Notice that the homogeneous equations of (3.5) have four localized solutions

$$(i\phi_1 \operatorname{sech} x, 0), \quad (0, i\phi_2 \operatorname{sech} x),$$

$$(\phi_2 \operatorname{sech} x, -\phi_1 \operatorname{sech} x) \quad \text{and} \quad (\phi_1 \operatorname{sech} x \tanh x, \phi_2 \operatorname{sech} x \tanh x).$$

In order for (3.5) to have a localized solution for A_1 and B_1 , the compatibility conditions need to be satisfied. These conditions are

$$\int_{-\infty}^{\infty} (\phi_1 F_1 - \phi_1^* F_1^*) \operatorname{sech} x dx = 0, \quad (3.7a)$$

$$\int_{-\infty}^{\infty} (\phi_2 F_2 - \phi_2^* F_2^*) \operatorname{sech} x dx = 0, \quad (3.7b)$$

$$\int_{-\infty}^{\infty} (\phi_2 F_1 + \phi_2^* F_1^* - \phi_1 F_2 - \phi_1^* F_2^*) \operatorname{sech} x dx = 0, \quad (3.7c)$$

$$\int_{-\infty}^{\infty} (\phi_1 F_1 + \phi_1^* F_1^* + \phi_2 F_2 + \phi_2^* F_2^*) \operatorname{sech} x \tanh x dx = 0. \quad (3.7d)$$

The condition (3.7d) is satisfied automatically because the functions F_1 and F_2 are even. When (3.6a) and (3.6b) are substituted into (3.7a), (3.7b) and (3.7c), the compatibility conditions are reduced to

$$\operatorname{Im} \{ \phi_1 (i\phi_{1T} + k\phi_2 + \frac{2}{3}b|\phi_2|^2 \phi_1) \} = 0, \quad (3.8a)$$

$$\operatorname{Im} \{ \phi_2 (i\phi_{2T} + k\phi_1 + \frac{2}{3}b|\phi_1|^2 \phi_2) \} = 0, \quad (3.8b)$$

$$\operatorname{Re} \{ \phi_2 (i\phi_{1T} + k\phi_2 + \frac{2}{3}b|\phi_2|^2 \phi_1) \} = \operatorname{Re} \{ \phi_1 (i\phi_{2T} + k\phi_1 + \frac{2}{3}b|\phi_1|^2 \phi_2) \}. \quad (3.8c)$$

It is easy to show that equations (3.8a), (3.8b) and (3.8c), together with (3.4), are equivalent to the two equations

$$i\phi_{1T} + k\phi_2 + \frac{2}{3}b|\phi_2|^2\phi_1 = 0, \quad (3.9a)$$

$$i\phi_{2T} + k\phi_1 + \frac{2}{3}b|\phi_1|^2\phi_2 = 0 \quad (3.9b)$$

which completely determine the slow-time evolution of the complex amplitudes $\phi_1(T)$ and $\phi_2(T)$. When ϕ_1 and ϕ_2 satisfy the equations (3.9), localized solutions A_1 and B_1 of the inhomogeneous equations (3.5) exist and can be determined straightforwardly. Higher order terms in the expansion (3.3) and higher order corrections to ϕ_1 and ϕ_2 can be obtained by carrying out the above multiple-scale analysis to higher orders.

Equations (3.9) can be solved exactly in terms of the Jacobian elliptic functions. Write

$$\phi_1 = r_1 e^{i\theta_1}, \quad \phi_2 = r_2 e^{i\theta_2} \quad (3.10)$$

where r_1, r_2 are non-negative and θ_1, θ_2 real. Equations (3.9) now become a system of four real-valued equations

$$r_{1T} = -kr_2 \sin(\theta_2 - \theta_1), \quad (3.11a)$$

$$r_{2T} = kr_1 \sin(\theta_2 - \theta_1), \quad (3.11b)$$

$$r_1\theta_{1T} = kr_2 \cos(\theta_2 - \theta_1) + \frac{2}{3}br_2^2r_1, \quad (3.11c)$$

$$r_2\theta_{2T} = kr_1 \cos(\theta_2 - \theta_1) + \frac{2}{3}br_1^2r_2. \quad (3.11d)$$

Equations (3.11) have a first integral

$$r_1^2 + r_2^2 = 2 \quad (3.12)$$

in view of equation (3.4). A little algebra reveals that they also have another first integral

$$r_1 r_2 \left\{ k \cos(\theta_2 - \theta_1) + \frac{1}{3} b r_1 r_2 \right\} = \text{constant} \equiv L. \quad (3.13)$$

Let $f = r_1^2 - 1$. By making use of these two first integrals, it can be shown that f satisfies the equation

$$f_T^2 = \frac{4}{9}b^2(\gamma + f^2)(\omega^2 - f^2) \quad (3.14)$$

where

$$\gamma = \frac{9}{2b^2}(|k|\sqrt{k^2 + \frac{4}{3}bL} + k^2 + \frac{2}{3}bL) - 1, \quad (3.15)$$

$$\omega^2 = \frac{9}{2b^2}(|k|\sqrt{k^2 + \frac{4}{3}bL} - k^2 - \frac{2}{3}bL) + 1 \quad (> 0). \quad (3.16)$$

The solution f is a periodic function and can be expressed in terms of the Jacobian elliptic functions. The exact forms of f and r_1^2 depend on the sign of γ . Suppose the initial condition for r_1 is $r_1 = r_{10}$ at $T = T_0$.

1. When $\gamma > 0$, the solution r_1^2 is

$$r_1^2 = 1 + \omega \operatorname{cn}\left\{\pm \frac{2}{3}|b|\sqrt{\gamma + \omega^2}(T - T_0) - C_1, m\right\}, \quad (3.17)$$

where $C_1 = \operatorname{cn}^{-1}\{(r_{10}^2 - 1)/\omega, m\}$, $m^2 = \omega^2/(\gamma + \omega^2)$ and $m > 0$. The sign “+” or “-” depends on the initial condition $\theta_2 - \theta_1$ and can be easily determined from equation (3.11a).

2. When $\gamma < 0$, the solution is

$$r_1^2 = 1 \pm \omega \sqrt{1 - m^2 \operatorname{sn}^2\left\{\pm \frac{2}{3}|b\omega|(T - T_0) - C_2, m\right\}} \quad (3.18)$$

where $C_2 = \operatorname{sn}^{-1}(\sqrt{\{\omega^2 - (r_{10}^2 - 1)^2\}/(\omega^2 + \gamma)}, m)$, $m^2 = (\omega^2 + \gamma)/\omega^2$, and the signs “+” or “-” depend on the initial conditions and can be easily determined.

After r_1^2 has been found, r_2^2 can be easily obtained from equation (3.12).

For demonstration purposes, let us consider a special initial condition of equations (3.9), $\phi_1(0) = \sqrt{2}$ and $\phi_2(0) = 0$, i.e. $r_1(0) = \sqrt{2}$, $\theta_1(0) = 0$, $r_2(0) = 0$ and $\theta_2(0) = 0$. In this case,

$$L = 0, \quad \gamma = \frac{9k^2}{b^2} - 1, \quad \omega^2 = 1. \quad (3.19)$$

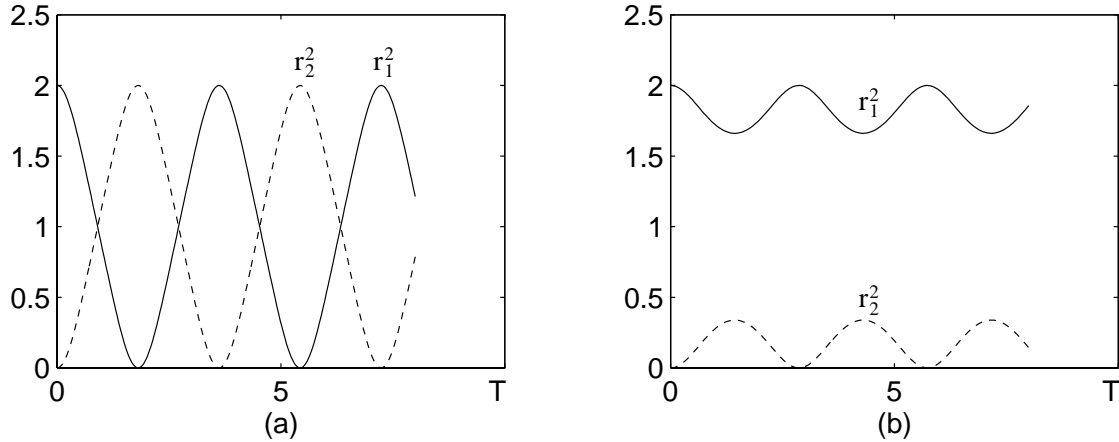


Figure 1: (a) r_1^2 and r_2^2 solutions (3.20) for $k = 1$ and $b = 2$. (b) r_1^2 and r_2^2 solutions (3.21) for $k = 0.5$ and $b = 2$.

1. If $|3k/b| > 1$, then $\gamma > 0$ and $m^2 = b^2/9k^2$. The solutions are

$$r_1^2 = 1 + \operatorname{cn}\left(2|k|T, \left|\frac{b}{3k}\right|\right), \quad (3.20a)$$

$$r_2^2 = 1 - \text{cn}(2|k|T, |\frac{b}{3k}|). \quad (3.20b)$$

The graphs of r_1^2 and r_2^2 are illustrated in Figure 1 (a) with $k = 1$ and $b = 2$. It is observed that in this case, the energy is fully transferred from the A component to the B component, then it switches back to the A component. This process continues indefinitely. Equations (3.20) also show that when $|k|$ gets smaller, the period of the amplitude oscillation will get larger.

2. If $|3k/b| < 1$, then $\gamma < 0$, $m^2 = 9k^2/b^2$. Now the solutions are

$$r_1^2 = 1 + \sqrt{1 - \frac{9k^2}{b^2} \text{sn}^2(\frac{2}{3}|b|T, |\frac{3k}{b}|)}, \quad (3.21a)$$

$$r_2^2 = 1 - \sqrt{1 - \frac{9k^2}{b^2} \text{sn}^2(\frac{2}{3}|b|T, |\frac{3k}{b}|)}. \quad (3.21b)$$

Their graphs are illustrated in Figure 1 (b) with $k = 0.5$ and $b = 2$. Notice that in this case, only part of the energy in the A component is transferred to the B component. At any time the A component retains more energy than the other. Equations (3.21) also indicate that when $|k|$ decreases, the amount of energy transferred from the A to the B component is correspondingly reduced. But, the period of the amplitude oscillation becomes smaller, which is just the opposite of what happens in the case where $|3k/b| > 1$.

The above analytical results can be readily confirmed by numerically integrating equations (1.1) with κ small and β close to 1. For easy comparison with the results (3.20) and (3.21), we choose the initial condition as

$$A(x, 0) = \sqrt{2} \text{sech} x, \quad B(x, 0) = 0. \quad (3.22)$$

1. When $\kappa = 0.1$ and $\beta = 0.8$, numerical solutions of $|A(x, t)|$ and $|B(x, t)|$ are graphed in Figure 2 (a, b). They are localized, oscillating structures with energy fully switching between the two components. This is expected from the above analytical results. $|A(0, t)|^2$ and $|B(0, t)|^2$ are predicted from (3.20) to be

$$r_1^2 = 1 + \text{cn}(0.2t, \frac{2}{3}), \quad (3.23a)$$

$$r_2^2 = 1 - \text{cn}(0.2t, \frac{2}{3}). \quad (3.23b)$$

A comparison between (3.23) and the numerically obtained amplitudes $|A(0, t)|^2$ and $|B(0, t)|^2$ is shown in Figure 2 (c, d). There is good agreement between them.

2. When $\kappa = 0.05$ and $\beta = 0.8$, numerical solutions of $|A(x, t)|$ and $|B(x, t)|$ are graphed in Figure 3 (a, b). Notice that only part of the energy in the A component is transferred to the B component, which is expected. The predicted values for $|A(0, t)|^2$ and $|B(0, t)|^2$ are

$$r_1^2 = 1 + \sqrt{1 - \frac{9}{16} \text{sn}^2(\frac{0.4}{3}t, \frac{3}{4})}, \quad (3.24a)$$

$$r_2^2 = 1 - \sqrt{1 - \frac{9}{16} \operatorname{sn}^2\left(\frac{0.4}{3}t, \frac{3}{4}\right)}. \quad (3.24b)$$

A comparison between (3.24) and the numerically obtained amplitudes $|A(0, t)|^2$ and $|B(0, t)|^2$ is shown in Figure 3 (c, d). It is observed that solutions (3.24) correctly capture the qualitative features of $|A(0, t)|^2$ and $|B(0, t)|^2$, although the quantitative agreement is not satisfactory. If κ is smaller and β closer to 1, the quantitative agreement will be better.

3.2 Weakly Oscillating Structures

Another type of oscillating structure arises when κ is small and β is positive, but not close to 1. In these structures, the amplitudes of the A and B components are very different. The amplitude of the bigger component is hardly oscillating, while that of the smaller component is strongly oscillating. We call such structures weakly oscillating structures.

Suppose $\kappa = \epsilon \ll 1$. Then equations (1.1) can be rewritten as

$$iA_t + A_{xx} + (AA^* + \beta BB^*)A = -\epsilon B, \quad (3.25a)$$

$$iB_t + B_{xx} + (BB^* + \beta AA^*)B = -\epsilon A. \quad (3.25b)$$

We seek weakly oscillating structures which have the following perturbation expansion

$$A(x, t) = A_0(x, t) + \epsilon^2 A_2(x, t) + \epsilon^4 A_4(x, t) + \dots, \quad (3.26a)$$

$$B(x, t) = \epsilon B_1(x, t) + \epsilon^3 B_3(x, t) + \dots \quad (3.26b)$$

At order 1,

$$iA_{0t} + A_{0xx} + A_0^2 A_0^* = 0. \quad (3.27)$$

For simplicity, we choose

$$A_0 = \sqrt{2} \operatorname{sech} x e^{it}. \quad (3.28)$$

At order ϵ , it is found that

$$iB_{1t} + B_{1xx} + 2\beta \operatorname{sech}^2 x B_1 = -\sqrt{2} \operatorname{sech} x e^{it}. \quad (3.29)$$

We can write the solution B_1 as

$$B_1(x, t) = C_1 \phi(x) e^{i\omega t} + \psi(x) e^{it} \quad (3.30)$$

where C_1 is a complex constant, $\phi(x) e^{i\omega t}$ is a homogeneous solution, $\psi(x) e^{it}$ is a non-homogeneous solution, and ω is a parameter to be determined so that $\phi(x)$ is a localized function. We also require that the functions $\phi(x)$ and $\psi(x)$ are real-valued. It is easy to show that $\phi(x)$ and $\psi(x)$ satisfy the equations

$$\phi_{xx} + (2\beta \operatorname{sech}^2 x - \omega) \phi = 0, \quad (3.31)$$

$$\psi_{xx} + (2\beta \operatorname{sech}^2 x - 1) \psi = -\sqrt{2} \operatorname{sech} x. \quad (3.32)$$

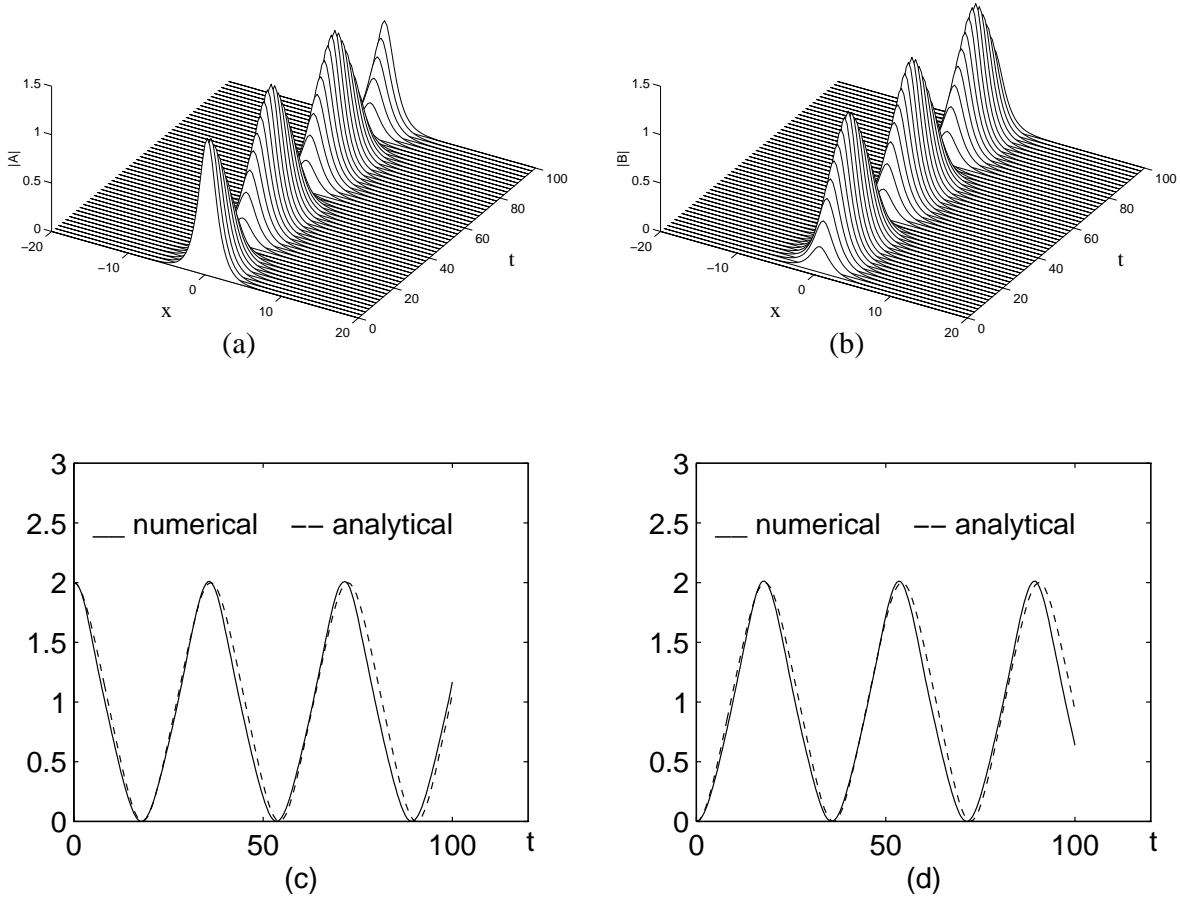


Figure 2: Numerical solutions of equations (1.1) with $\kappa = 0.1$ and $\beta = 0.8$. (a) $|A(x,t)|$ evolution; (b) $|B(x,t)|$ evolution; (c) $|A(0,t)|^2$ compared with the perturbative approximation (3.20a); (d) $|B(0,t)|^2$ compared with the perturbative approximation (3.20b).

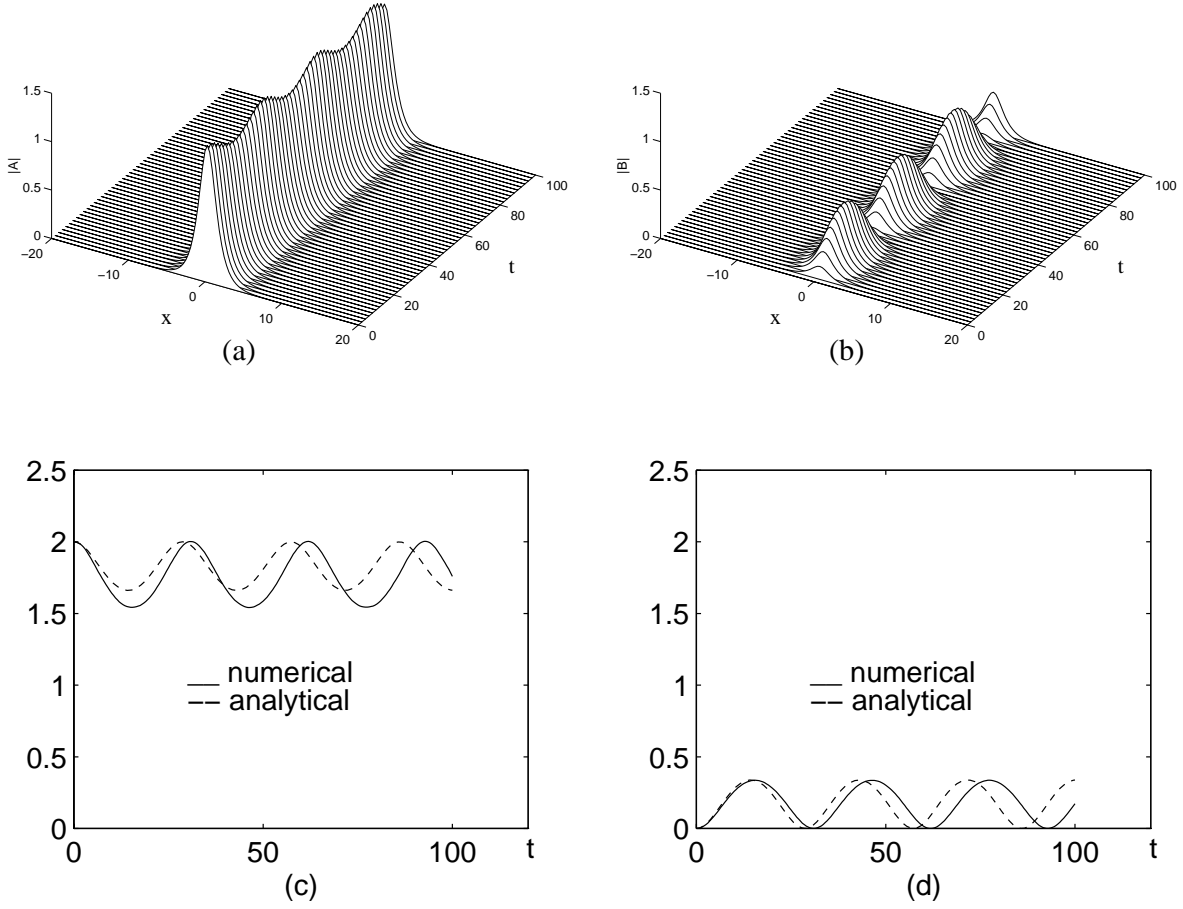


Figure 3: Numerical solutions of equations (1.1) with $\kappa = 0.05$ and $\beta = 0.8$. (a) $|A(x,t)|$ evolution; (b) $|B(x,t)|$ evolution; (c) $|A(0,t)|^2$ compared with the perturbative approximation (3.21a); (d) $|B(0,t)|^2$ compared with the perturbative approximation (3.21b).

Equation (3.31) can be solved analytically ([3]). It may have more than one localized solution for $\phi(x)$ depending on the value of β . For simplicity, we choose the lowest-mode solution

$$\phi(x) = \operatorname{sech}^s x, \quad \omega = s^2, \quad (3.33)$$

where $s = (\sqrt{1+8\beta}-1)/2$. Another reason for this choice is that higher-mode solutions $\phi(x)$ tend to make (3.26) unstable and lead to its disintegration. When $\beta \neq 1$, equation (3.32) always has a unique localized and symmetric solution $\psi(x)$. This solution can be readily determined numerically if β is specified. For instance, when $\beta = 1.5$, $\psi(x)$ is plotted in Figure 4.

It now becomes clear that for the solutions (3.26), to the leading order, the amplitude of the A component $|A(x, t)| \approx \sqrt{2}\operatorname{sech}x$ remains unchanged with time. On the other hand, the amplitude of the B component is

$$|B(x, t)| \approx |\kappa| |C_1 \phi(x) e^{i(\omega-1)t} + \psi(x)|, \quad (3.34)$$

which changes periodically with time. The period is $2\pi/|\omega-1|$. If $\beta = 1.5$, then $s = (\sqrt{13}-1)/2 \approx 1.30$, $\omega = s^2 \approx 1.70$, $\phi(x) = \operatorname{sech}^s x$, and $\psi(x)$ is as shown in Figure 4. For the choice $C_1 = 2$, the evolution of $|C_1 \phi(x) e^{i(\omega-1)t} + \psi(x)|$ is illustrated in Figure 5.

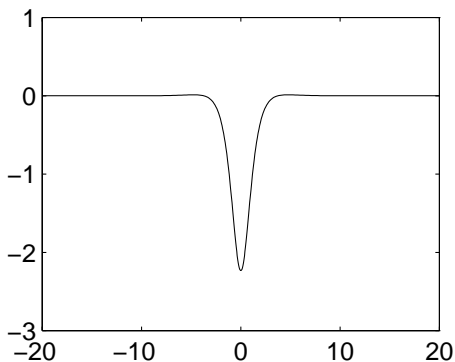


Figure 4: The solution $\psi(x)$ of the equation (3.32) for $\beta = 1.5$.

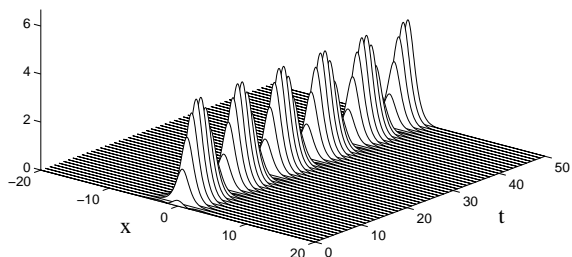


Figure 5: Evolution of $|\psi(x) + C_1 \phi(x) e^{i(\omega-1)t}|$ for $\beta = 1.5$ and $C_1 = 2$.

The weakly oscillating structures (3.26) often appear in the system (1.1) when κ is small, $\beta > 0$ but not close to 1 and initially the amplitudes of A and B are very different. For instance, when $\kappa = 0.1$, $\beta = 1.5$, and initially $A(x, 0) = \sqrt{2}\operatorname{sech}x$, $B(x, 0) = 0$, the numerical solutions of equations (1.1) are shown in Figure 6 (a, b). It can be observed that $|A(x, t)|$ is much larger than $|B(x, t)|$ and is hardly oscillating, while $|B(x, t)|$ is strongly oscillating. The oscillation period of $|B(x, t)|$ is about 9.5, which can be compared to the analytically predicted value $2\pi/|\omega-1| \approx 9.0$ (to the leading order). Figure 6 (c) plots the amplitudes $|A(0, t)|$ and $|B(0, t)|$ against time. Figure 6 (d) plots the temporal spectra of $A(0, t)$ and $B(0, t)$. It can be observed that $A(0, t)$ has a dominant frequency which is about 1.06, and $B(0, t)$ has two dominant frequencies which are around 1.06 and 1.72. These results agree well with the perturbation results presented above.

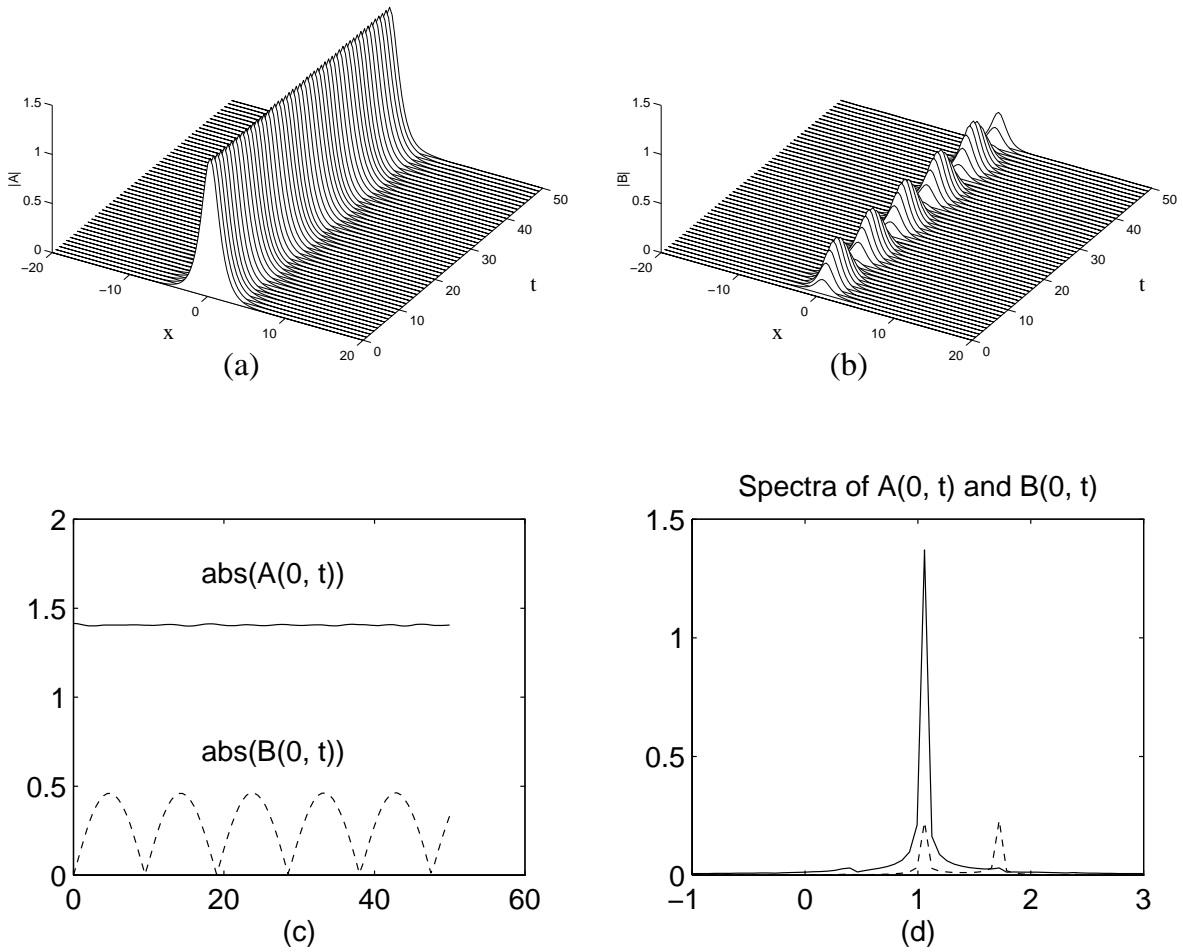


Figure 6: Numerical solutions of equations (1.1) with $\kappa = 0.1$ and $\beta = 1.5$. (a) $|A(x, t)|$ evolution; (b) $|B(x, t)|$ evolution; (c) $|A(0, t)|$ and $|B(0, t)|$; (d) temporal spectra of $A(0, t)$ (solid) and $B(0, t)$ (dashed).

The higher order terms in the perturbation series (3.26) contain further important information about these weakly oscillating structures. At order ϵ^2 , denoting $A_2(x, t) = e^{it}a_2(x, t)$, it is found that a_2 is governed by the equation

$$ia_{2t} + a_{2xx} - a_2 + 4\text{sech}^2xa_2 + 2\text{sech}^2xa_2^* = w_0(x) + C_1w_1(x)e^{i(\omega-1)t} + C_1^*w_2(x)e^{-i(\omega-1)t}, \quad (3.35)$$

where

$$w_0(x) = -\psi(x) - \sqrt{2}\beta(|C_1|^2\phi^2 + \psi^2)\text{sech}x, \quad (3.36a)$$

$$w_1(x) = -\phi(1 + \sqrt{2}\beta\psi\text{sech}x), \quad (3.36b)$$

$$w_2(x) = -\sqrt{2}\beta\phi\psi\text{sech}x \quad (3.36c)$$

are real-valued functions. The solution a_2 can be written as

$$a_2(x, t) = u_0(x) + C_1u_1(x)e^{i(\omega-1)t} + C_1^*u_2(x)e^{-i(\omega-1)t}, \quad (3.37)$$

where $u_0(x), u_1(x), u_2(x)$ are real-valued functions and satisfy the following equations:

$$u_{0xx} - u_0 + 6\text{sech}^2xu_0 = w_0, \quad (3.38)$$

$$u_{1xx} - \omega u_1 + 4\text{sech}^2xu_1 + 2\text{sech}^2xu_2 = w_1, \quad (3.39a)$$

$$u_{2xx} - (2 - \omega)u_2 + 4\text{sech}^2xu_2 + 2\text{sech}^2xu_1 = w_2. \quad (3.39b)$$

u_0 has a localized solution, since the compatibility condition

$$\int_{-\infty}^{\infty} w_0(x)\text{sech}x \tanh x \, dx = 0 \quad (3.40)$$

is satisfied. The determination of u_0 is straightforward. u_1 and u_2 's behaviors are different and need further investigation.

First we discuss the case $\omega > 2$, i.e. $\beta > 1 + \sqrt{2}/2 \approx 1.7071$.

When $\omega > 2$, the homogeneous equations of (3.39) have two linearly independent solutions which are bounded at infinity: one is symmetric and denoted as $(u_{1h}^{(s)}, u_{2h}^{(s)})$, and the other one is anti-symmetric and denoted as $(u_{1h}^{(a)}, u_{2h}^{(a)})$. At infinity, $u_{1h}^{(s)}$ and $u_{1h}^{(a)}$ exponentially decay, but $u_{2h}^{(s)}$ and $u_{2h}^{(a)}$ are oscillatory. The asymptotic behaviors of these two homogeneous solutions are

$$u_{1h}^{(s)} \longrightarrow c_1 e^{-\sqrt{\omega}|x|}, \quad x \longrightarrow \infty, \quad (3.41a)$$

$$u_{2h}^{(s)} \longrightarrow c_2 \text{sgn}(x) \sin \sqrt{\omega-2}x + c_3 \cos \sqrt{\omega-2}x, \quad x \longrightarrow \infty, \quad (3.41b)$$

$$u_{1h}^{(a)} \longrightarrow d_1 \text{sgn}(x) e^{-\sqrt{\omega}|x|}, \quad x \longrightarrow \infty, \quad (3.42a)$$

$$u_{2h}^{(a)} \longrightarrow d_2 \sin \sqrt{\omega-2}x + d_3 \text{sgn}(x) \cos \sqrt{\omega-2}x, \quad x \longrightarrow \infty. \quad (3.42b)$$

If these solutions are normalized by the conditions

$$c_1 > 0, \quad c_2^2 + c_3^2 = 1, \quad (3.43a)$$

$$d_1 > 0, \quad d_2^2 + d_3^2 = 1, \quad (3.43b)$$

then they will be unique. The normalized solutions are denoted as $(\hat{u}_{1h}^{(s)}, \hat{u}_{2h}^{(s)})$ and $(\hat{u}_{1h}^{(a)}, \hat{u}_{2h}^{(a)})$. They can be effectively determined by numerical methods. A localized solution (u_1, u_2) for the inhomogeneous equations (3.39) exists only if the compatibility conditions

$$\int_{-\infty}^{\infty} (w_1 \hat{u}_{1h}^{(s)} + w_2 \hat{u}_{2h}^{(s)}) dx = 0, \quad (3.44a)$$

$$\int_{-\infty}^{\infty} (w_1 \hat{u}_{1h}^{(a)} + w_2 \hat{u}_{2h}^{(a)}) dx = 0 \quad (3.44b)$$

are satisfied. In the present case, w_1 and w_2 are symmetric functions, so condition (3.44b) is automatically satisfied. But condition (3.44a), in general, is not. This indicates that any (u_1, u_2) solution of equations (3.39), which is bounded at infinity, is such that u_1 is localized, but u_2 has an oscillating tail at infinity with wavenumbers $\pm\sqrt{\omega-2}$. We can further determine the amplitude of this infinite oscillating tail. Let us consider a symmetric solution $(u_1^{(s)}, u_2^{(s)})$ of equations (3.39). Suppose its asymptotic behavior at infinity is

$$u_1^{(s)} \longrightarrow h_1 e^{-\sqrt{\omega}|x|}, \quad x \longrightarrow \infty, \quad (3.45a)$$

$$u_2^{(s)} \longrightarrow h_2 \operatorname{sgn}(x) \sin \sqrt{\omega-2} x + h_3 \cos \sqrt{\omega-2} x, \quad x \longrightarrow \infty. \quad (3.45b)$$

By adding a suitable symmetric homogeneous solution $(u_{1h}^{(s)}, u_{2h}^{(s)})$ to $(u_1^{(s)}, u_2^{(s)})$, we can make $h_3 = 0$. Then a little algebra shows that

$$\int_{-\infty}^{\infty} (w_1 \hat{u}_{1h}^{(s)} + w_2 \hat{u}_{2h}^{(s)}) dx = 2\sqrt{\omega-2} c_3 h_2, \quad (3.46)$$

by which the amplitude of the oscillating tail h_2 can be determined. It should be noted that this infinite oscillating tail can not be suppressed by introducing multiple temporal and spatial scales in the expansion (3.26). Rather, it is an integral part in this perturbation solution.

Next we apply the above general results to a special case $\beta = 2$. In this case, $\omega = (\sqrt{17} - 1)^2/4 \approx 2.4384$. The normalized homogeneous solutions $(\hat{u}_{1h}^{(s)}, \hat{u}_{2h}^{(s)})$ and $(\hat{u}_{1h}^{(a)}, \hat{u}_{2h}^{(a)})$ are numerically determined and plotted in Figure 7. The coefficients c_i, d_i ($i = 1, 2, 3$) in their asymptotic behaviors at infinity (3.41) and (3.42) are found to be

$$c_1 = 0.0043, \quad c_2 = -0.9207, \quad c_3 = 0.3904, \quad (3.47a)$$

$$d_1 = 0.0014, \quad d_2 = 0.3904, \quad d_3 = 0.9207. \quad (3.47b)$$

The function $\phi(x)$ is equal to $\operatorname{sech}^s x$ where $s = (\sqrt{17} - 1)/2 \approx 1.5616$, and $\psi(x)$ is numerically determined and plotted in Figure 8. The corresponding functions $w_1(x)$ and $w_2(x)$, as determined by (3.36), are plotted in Figure 9. It is found numerically that

$$\int_{-\infty}^{\infty} (w_1 \hat{u}_{1h}^{(s)} + w_2 \hat{u}_{2h}^{(s)}) dx = -1.6302 \neq 0, \quad (3.48)$$

which indicates that any solution (u_1, u_2) of equations (3.39) is not localized. Rather, u_2 has an oscillating tail at infinity. For a symmetric solution $(u_1^{(s)}, u_2^{(s)})$ whose asymptotic behavior is

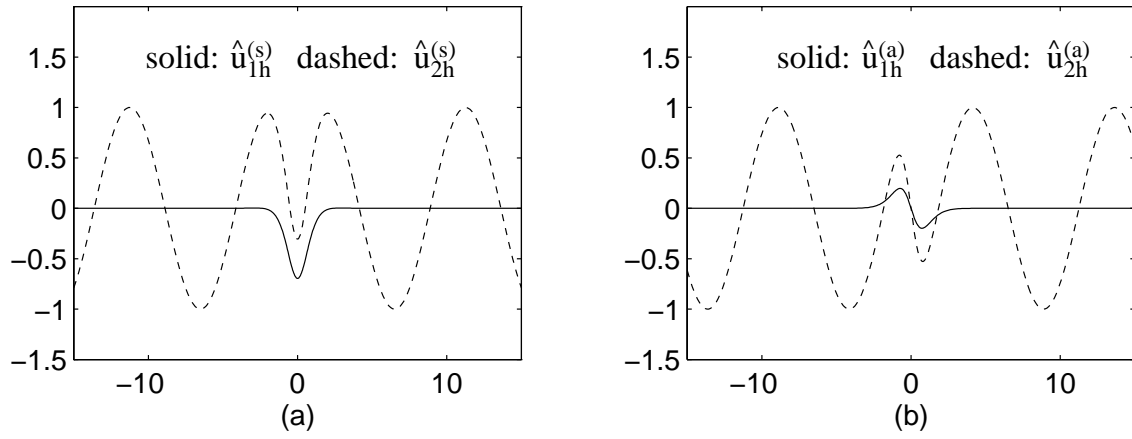


Figure 7: The two normalized homogeneous solutions of equations (3.39). (a) the symmetric solution $(\hat{u}_{1h}^{(s)}, \hat{u}_{2h}^{(s)})$; (b) the anti-symmetric solution $(\hat{u}_{1h}^{(a)}, \hat{u}_{2h}^{(a)})$.

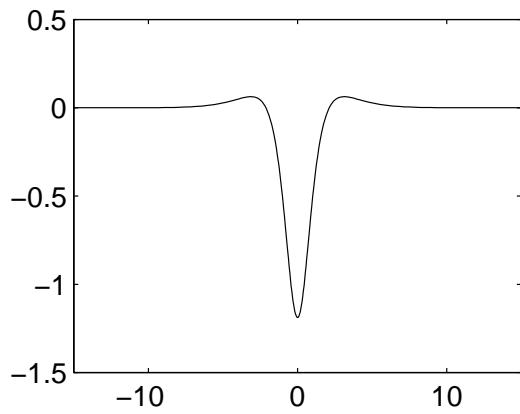


Figure 8: The solution $\psi(x)$ of the equation (3.32) for $\beta = 2$.

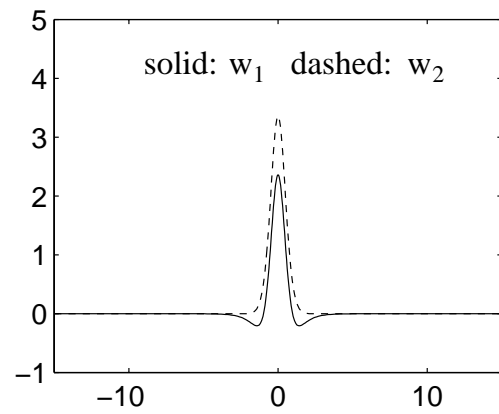


Figure 9: $w_1(x)$ and $w_2(x)$ (as given by (3.36)) for $\beta = 2$.

given by (3.45), if $h_3 = 0$, then the size of the oscillating tail h_2 is determined by (3.46) to be $h_2 = -3.1531$.

When $0 < \omega < 2$, i.e. $0 < \beta < 1 + \sqrt{2}/2 \approx 1.7071$, there are no homogeneous solutions of equations (3.39) which are bounded at infinity unless $\omega = 1$, i.e. $\beta = 1$. In the current assumption, β is not close to 1. So a unique localized solution (u_1, u_2) of equations (3.39) exists. This indicates that a localized solution for $A_2(x, t)$ can be successfully constructed. But some more calculations quickly reveal that oscillating tails arise in higher order terms in the perturbation expansion (3.26).

The appearance of infinite oscillating tails in the solution (3.26) shows that (3.26) is not a strictly localized solution of equations (3.25). It indicates that the localized weakly oscillating structure

$$A = A_0 = \sqrt{2} \operatorname{sech} x e^{it}, \quad (3.49a)$$

$$B = \epsilon B_1 = \epsilon (C_1 \phi(x) e^{i\omega t} + \psi(x) e^{it}) \quad (3.49b)$$

in equations (3.25) will develop infinite oscillating tails and transfer energy into them. This leads to the energy dissipation of this structure. If ϵ is small, then the oscillating tails are very small in size, which implies that the dissipation of energy in (3.49) is very weak. So this localized structure can remain localized for a long time, just as in Figure 6. Nonetheless, it is unstable and steadily loses its energy. It is not clear now whether this structure will lose all its energy and eventually disappear, or it will slowly readjust its shape, shedding off part of its energy, and reach a stable vector soliton or localized oscillating state. This question will be considered elsewhere.

The reason why infinite oscillating tails appear in the perturbation expansion (3.26) is clear from the above analysis. Generally speaking, it is due to nonlinearity in the underlying wave equations and the involvement of more than one dominant frequency in the solutions. There is reason to suggest that in other similar situations, these tails will arise in a similar fashion. One example will be given in the next subsection.

The infinite oscillating tails in the perturbed KdV equation bear some resemblance to those in the solution (3.26) for the perturbed equations (3.25) ([11], [12]). But, some differences need to be pointed out. In the former case, the tails are very short waves and their amplitudes exponentially small; while in the latter, the tails are not short waves and their amplitudes are only algebraically small. In the former case, the oscillating tails are anticipated from the equation's linear dispersion relation; while they are not in the latter.

3.3 Oscillating Structures with Two Dominant Frequencies

When β is close to 1 but κ not small, oscillating structures with two dominant frequencies exist. Suppose $\beta = 1 + \epsilon b$, then equations (1.1) can be reorganized as

$$iA_t + A_{xx} + \kappa B + (AA^* + BB^*)A = -\epsilon b BB^* A, \quad (3.50a)$$

$$iB_t + B_{xx} + \kappa A + (BB^* + AA^*)B = -\epsilon bAA^*B. \quad (3.50b)$$

A change of variables

$$A = \frac{1}{\sqrt{2}}(Ue^{i\kappa t} + Ve^{-i\kappa t}), \quad B = \frac{1}{\sqrt{2}}(Ue^{i\kappa t} - Ve^{-i\kappa t}) \quad (3.51)$$

reduces equations (3.50) to the following form:

$$iU_t + U_{xx} + (UU^* + VV^*)U = -\frac{1}{2}\epsilon b(U^2 - V^2e^{-4i\kappa t})U^*, \quad (3.52a)$$

$$iV_t + V_{xx} + (VV^* + UU^*)V = -\frac{1}{2}\epsilon b(V^2 - U^2e^{4i\kappa t})V^*. \quad (3.52b)$$

When $\epsilon = 0$,

$$U(x, t) = \phi_1 \operatorname{sech} x e^{it}, \quad V(x, t) = \phi_2 \operatorname{sech} x e^{it} \quad (3.53)$$

are solutions of (3.52), where ϕ_1 and ϕ_2 are complex constants and $|\phi_1|^2 + |\phi_2|^2 = 2$. When ϵ is non-zero but small, solutions can be expanded as the following perturbation series

$$U = e^{it} \{ \phi_1(T) \operatorname{sech} x + \epsilon U_1(x, t, T, \epsilon) + \dots \}, \quad (3.54a)$$

$$V = e^{it} \{ \phi_2(T) \operatorname{sech} x + \epsilon V_1(x, t, T, \epsilon) + \dots \} \quad (3.54b)$$

where $T = \epsilon t$ is the slow-time scale and

$$|\phi_1(T)|^2 + |\phi_2(T)|^2 = 2. \quad (3.55)$$

Notice that the corresponding A, B solutions have two dominant frequencies $1 + \kappa$ and $1 - \kappa$.

At order ϵ ,

$$iU_{1t} + U_{1xx} - U_1 + \{(2|\phi_1|^2 + |\phi_2|^2)U_1 + \phi_1^2 U_1^* + \phi_1 \phi_2^* V_1 + \phi_1 \phi_2 V_1^*\} \operatorname{sech}^2 x = F_1, \quad (3.56a)$$

$$iV_{1t} + V_{1xx} - V_1 + \{(2|\phi_2|^2 + |\phi_1|^2)V_1 + \phi_2^2 V_1^* + \phi_2 \phi_1^* U_1 + \phi_1 \phi_2 U_1^*\} \operatorname{sech}^2 x = F_2, \quad (3.56b)$$

where

$$F_1 = -i\phi_{1T} \operatorname{sech} x - \frac{1}{2}b\phi_1^2 \phi_1^* \operatorname{sech}^3 x + \frac{1}{2}b\phi_2^2 \phi_1^* \operatorname{sech}^3 x e^{-4i\kappa t}, \quad (3.57a)$$

$$F_2 = -i\phi_{2T} \operatorname{sech} x - \frac{1}{2}b\phi_2^2 \phi_2^* \operatorname{sech}^3 x + \frac{1}{2}b\phi_1^2 \phi_2^* \operatorname{sech}^3 x e^{4i\kappa t}. \quad (3.57b)$$

The solutions U_1, V_1 can be written as

$$U_1(x, t) = u_0(x) + u_1(x)e^{4i\kappa t} + u_2(x)e^{-4i\kappa t}, \quad (3.58a)$$

$$V_1(x, t) = v_0(x) + v_1(x)e^{4i\kappa t} + v_2(x)e^{-4i\kappa t}, \quad (3.58b)$$

where $u_i(x), v_i(x) (i = 0, 1, 2)$ are complex functions. u_0, v_0 satisfy the equations

$$u_{0xx} - u_0 + \{(2|\phi_1|^2 + |\phi_2|^2)u_0 + \phi_1^2 u_0^* + \phi_1 \phi_2^* v_0 + \phi_1 \phi_2 v_0^*\} \operatorname{sech}^2 x = -i\phi_{1T} \operatorname{sech} x - \frac{1}{2}b\phi_1^2 \phi_1^* \operatorname{sech}^3 x, \quad (3.59a)$$

$$v_{0xx} - v_0 + \{(2|\phi_2|^2 + |\phi_1|^2)v_0 + \phi_2^2 v_0^* + \phi_2 \phi_1^* u_0 + \phi_1 \phi_2 u_0^*\} \operatorname{sech}^2 x = -i\phi_{2T} \operatorname{sech} x - \frac{1}{2}b\phi_2^2 \phi_2^* \operatorname{sech}^3 x. \quad (3.59b)$$

In order for (3.59) to have localized solutions for u_0 and v_0 , similar compatibility conditions as those in Section 3.1 conclude that

$$i\phi_{1T} + \frac{1}{3}b\phi_1^2\phi_1^* = 0, \quad (3.60a)$$

$$i\phi_{2T} + \frac{1}{3}b\phi_2^2\phi_2^* = 0. \quad (3.60b)$$

The solutions of (3.60) are

$$\phi_1(T) = |\phi_1(0)|\exp\left\{\frac{1}{3}ib|\phi_1(0)|^2T\right\}, \quad (3.61a)$$

$$\phi_2(T) = |\phi_2(0)|\exp\left\{\frac{1}{3}ib|\phi_2(0)|^2T\right\}. \quad (3.61b)$$

So the amplitudes $|\phi_1(T)|$ and $|\phi_2(T)|$ do not change with time. With ϕ_1 and ϕ_2 thus given, localized solutions (u_0, v_0) of equations (3.59) exist and can be determined straightforwardly. The functions $u_i, v_i (i = 1, 2)$ satisfy the equations

$$u_{1xx} - (1 + 4\kappa)u_1 + \{(2|\phi_1|^2 + |\phi_2|^2)u_1 + \phi_1^2u_2^* + \phi_1\phi_2^*v_1 + \phi_1\phi_2v_2^*\}\operatorname{sech}^2x = 0, \quad (3.62a)$$

$$v_{1xx} - (1 + 4\kappa)v_1 + \{(2|\phi_2|^2 + |\phi_1|^2)v_1 + \phi_2^2v_2^* + \phi_2\phi_1^*u_1 + \phi_1\phi_2u_2^*\}\operatorname{sech}^2x = \frac{1}{2}b\phi_1^2\phi_2^*\operatorname{sech}^3x, \quad (3.62b)$$

$$u_{2xx} - (1 - 4\kappa)u_2 + \{(2|\phi_1|^2 + |\phi_2|^2)u_2 + \phi_1^2u_1^* + \phi_1\phi_2^*v_2 + \phi_1\phi_2v_1^*\}\operatorname{sech}^2x = \frac{1}{2}b\phi_2^2\phi_1^*\operatorname{sech}^3x, \quad (3.62c)$$

$$v_{2xx} - (1 - 4\kappa)v_2 + \{(2|\phi_2|^2 + |\phi_1|^2)v_2 + \phi_2^2v_1^* + \phi_2\phi_1^*u_2 + \phi_1\phi_2u_1^*\}\operatorname{sech}^2x = 0. \quad (3.62d)$$

The situation now is similar to that for equations (3.39). When $\kappa > 1/4$, equations (3.62) in general do not have localized solutions. Rather, u_2 and v_2 have oscillating tails at infinity with wavenumbers $\sqrt{4\kappa - 1}$. Similarly, when $\kappa < -1/4$, u_1 and v_1 have oscillating tails at infinity. When $|\kappa| < 1/4$, oscillating tails will not arise at this order, but they will appear in the higher order terms in the expansion (3.54).

The appearance of infinite oscillating tails in the expansion (3.54) indicates that (3.54) is not a strictly localized solution of equations (3.52). This implies that the two-frequency soliton solutions

$$A = \frac{1}{\sqrt{2}}(\phi_1e^{i(1+\kappa)t} + \phi_2e^{i(1-\kappa)t})\operatorname{sech}x, \quad (3.63a)$$

$$B = \frac{1}{\sqrt{2}}(\phi_1e^{i(1+\kappa)t} - \phi_2e^{i(1-\kappa)t})\operatorname{sech}x \quad (3.63b)$$

of the undisturbed equations (3.50) (with $\epsilon = 0$), where complex constants ϕ_1 and ϕ_2 are such that $|\phi_1|^2 + |\phi_2|^2 = 2$, are unstable to cross-phase-modulational perturbations. The solitons (3.63) will develop infinite oscillating tails and lose their energy. Here again, the appearance of infinite oscillating tails is due to nonlinearity in equations (3.50) and two distinct frequencies in the leading order solutions (3.63), similar to the case discussed in the last subsection.

4 Summary

In the above two sections, both the vector solitons (permanent waves) and the oscillating structures in the wave system (1.1) have been studied. Previous analytical work has shown that only very special vector solitons are stable. Previous numerical work indicates that localized, oscillating structures often appear in the solutions. In the present work, focus has been put on these oscillating structures. Three types of such structures have been identified. Also, their detailed dynamics have been determined analytically using the perturbation techniques. The first type is a localized oscillating structure with a single dominant temporal frequency. They are able to remain localized for all times. The second and third types are oscillating structures which have more than one dominant frequency. They are not strictly localized since infinite oscillating tails are present. These structures, if initially localized, will gradually feed energy to the oscillating tails and evolve into some other stable states.

References

- [1] Zakharov, V.E. and Shabat, A.B. "Exact theory of two-dimensional self-focusing and one-dimensional self modulation of waves in nonlinear media." *Sov. Phys. JETP* 34, 62-69 (1972).
- [2] Menyuk, C. R. "Nonlinear pulse propagation in birefringent optical fibers." *IEEE J. Quantum Electron.* QE-23, 174 (1987).
- [3] Yang, J. and Benney, D. J. "Some properties of nonlinear wave systems." *Stud. Appl. Math.* 96, 111 (1996).
- [4] Kaup, D. J., Malomed, B. A. and Tasgal, R. S. "Internal dynamics of a vector soliton in a nonlinear optical fiber." *Phys. Rev. E* 48, 3049 (1993).
- [5] Ueda, T. and Kath, W.L. "Dynamics of coupled solitons in nonlinear optical fibers." *Phys. Rev. A* 42, 563-571 (1990).
- [6] Yang, J. "Vector solitons and their internal oscillations in birefringent nonlinear optical fibers." To appear in *Stud. Appl. Math.* (1996)
- [7] Wright, E.M., Stegeman, G.I. and Wabnitz, S. "Solitary-wave decay and symmetry-breaking instabilities in two-mode fibers." *Phys. Rev. A* 40, 4455-4466 (1989).
- [8] Akhmediev, N. N., Buryak, A. V., Soto-Crespo, J. M. and Andersen, D. R. "Phase-locked stationary soliton states in birefringent nonlinear optical fibers." *J. Opt. Soc. Am. B* 12, 434 (1995).
- [9] Blow, K. J., Doran, N. J. and Wood, D. "Polarization instabilities for solitons in birefringent fibers." *Opt. Lett.* 12, 202-204 (1987).
- [10] Chu, P. L., Malomed, B. A. and Peng, G. D. "Soliton switching and propagation in nonlinear fiber couplers: analytical results." *J. Opt. Soc. Am. B* 10, 1379 (1993).
- [11] Pomeau, Y., Ramani, A. and Grammaticos, B. "Structural stability of the Korteweg-de Vries solitons under a singular perturbation." *Phys. D* 31, 127-134 (1988).
- [12] Milewski, P. "Oscillating tails in the perturbed Korteweg-de Vries equation." *Stud. Appl. Math.* 90, 87-90 (1993).